

Statistical mechanics of a two-dimensional system with long-range interactions

This article has been downloaded from IOPscience. Please scroll down to see the full text article.

1998 J. Phys. A: Math. Gen. 31 3949

(<http://iopscience.iop.org/0305-4470/31/17/006>)

View [the table of contents for this issue](#), or go to the [journal homepage](#) for more

Download details:

IP Address: 171.66.16.121

The article was downloaded on 02/06/2010 at 06:36

Please note that [terms and conditions apply](#).

Statistical mechanics of a two-dimensional system with long-range interactions

David S Dean[†] and Giorgio Parisi[‡]

[†] CNRS-Laboratoire de Physique Théorique de l'Ecole Normale Supérieure, 24 rue Lhomond, F-75231, Paris Cedex 05, France

[‡] Dipartimento di Fisica and INFN, Università di Roma, La Sapienza, P A Moro 2, 00185 Roma, Italy

Received 11 November 1997

Abstract. We analyse the statistical physics of a two-dimensional lattice-based system with long-range interactions. The particles interact in a way analogous to the queens on a chess board. The long-range nature of the interaction gives the mathematics of the problem a simple geometric structure which simplifies both the analytic and numerical study of the system. We present some analytic calculations for the statics of the problem and we also perform Monte Carlo simulations which exhibit a dynamical transition between a high-temperature liquid regime and a low-temperature glassy regime exhibiting ageing in the two time-correlation functions.

1. Introduction

It is believed that one of the essential elements for the formation of a glassy phase is the presence of frustration along with a large number of metastable states. The glass transition is a dynamical one; if one considers ordinary glass one sees the glass phase because on rapid cooling the system does not manage to find the crystalline structure of silicon dioxide. Instead, the system becomes trapped on experimental timescales in a state of higher energy than the crystalline state. This phase is characterized by very slow dynamics and often exhibits ageing phenomena in many observable quantities such as the correlation and response functions. A good introduction to the problem of the glass transition may be found in [1]. Much of the understanding of glassy or out-of-equilibrium dynamics has been made via analogy with the dynamics of spin glasses and other systems with quenched disorder (for a review see [5]). Ideas from the theory of spin glasses have been tentatively put forward to understand the glass transition [3]. In this paper we put forward a new model, which we hope will be of use as a test of these ideas on systems without quenched disorder. We will emphasize its attractiveness as a model from both analytic and simulational points of view.

A well known puzzle to chess players is the eight queens problem. On a standard chess board it may be summarized as the problem of arranging eight queens such that no queen is in a position to take another queen at the next move. The interested reader will find that it is a non-trivial task to find such an arrangement. In this paper we will analyse a model based on the eight queens problem.

The attraction of this model is that the long-range nature of the interactions facilitates a rather straightforward and efficient implementation of Monte Carlo dynamics for computer

simulations. In addition we shall see that, whilst we cannot solve the statics exactly, various approximation schemes become analytically much simpler.

The space of the model is an $N \times N$ lattice with periodic boundary conditions imposed to facilitate analytic and numerical analysis; the original problem of course does not have periodic boundary conditions. On this lattice are N particles, the energy of a given configuration is given by the Hamiltonian

$$H = \sum_{i \neq j}^N \delta_{x_i, x_j}^N + \delta_{y_i, y_j}^N + \delta_{x_i - y_i, x_j - y_j}^N + \delta_{x_i + y_i, x_j + y_j}^N \quad (1)$$

where the position of the i th particle is denoted by the pair (x_i, y_i) . The superscript N on δ indicates that they are the standard Kronecker delta functions but with arithmetic modulo N . One can see that, for a periodic chess board, the solution of the eight queens problem is given by the zero-energy configurations of the Hamiltonian system above. The first two terms in the Hamiltonian represent the row and column constraints and the second two represent the constraint on the left-to-right and right-to-left diagonals respectively.

In certain cases it is rather easy to find the zero-energy states of the system. Let us consider the case where N is prime. As an ansatz we shall take the configuration

$$x_i = i \quad \text{and} \quad y_i = pi \quad (2)$$

for each i between 1 and N and where $0 < p < N$. Clearly the column constraint is satisfied automatically. To violate the row constraint we would have to have

$$p(i - j) \equiv 0 \quad (3)$$

where \equiv will always be taken to indicate equality modulo N , the fact that N is prime means that this may only be satisfied when $i \equiv j$. Violation of the first diagonal constraint would mean that

$$(p - 1)(i - j) \equiv 0. \quad (4)$$

This would imply that $i \equiv j$ or $p - 1 \equiv N$. Violation of the second diagonal constraint would imply

$$(p + 1)(i - j) \equiv 0 \quad (5)$$

hence either $i \equiv j$ or $p + 1 \equiv 0$. Therefore when one can find p such that $p + 1$ and $p - 1$ are not equal to zero modulo N , then the above construction does indeed give a zero-energy state. This analysis therefore demonstrates the existence of zero-energy states for all N primes strictly greater than 3.

This analysis is useful for our study of the dynamics; the ground states above are our analogy of the crystalline state of silicon dioxide when comparison is made with real glass.

2. Mean-field analysis

The queen's problem has a different algebraic structure depending on whether the lattice size N is even or odd, in the following analysis we shall consider the case N odd with the algebra being simplified because, in this case, perpendicular diagonals intersect only once. In the case where N is even, perpendicular diagonals cross either twice or not at all. To see this, without loss of generality, consider a diagonal (i, i) and a perpendicular diagonal $(j, c - j)$. At the intersection(s), $i \equiv j$ and $i \equiv c - j$, hence $2i \equiv c$. Consider now the case where N is odd: (1) if c is odd then $i = N/2 + c/2$ and is unique; if c is even then

$i = c/2$ and is unique. When N is even: (1) if c is odd then there is no solution and hence no intersection; (2) if c is even then $i = N/2 + c/2$ and $i = c/2$ are solutions.

One may carry out a geometrical mean-field Boltzmann-type analysis to determine the energy per particle of the system. Consider the configuration about one particle at the point O which is fixed. Ignoring the effects of correlations, the particle at O has two types of sites surrounding it: those with which it interacts directly, i.e. those which are on the same row, column or diagonal which we shall call type A , and those with which it does not interact directly which we shall call type B . Denote by $N_{X \rightarrow Y}$ the number of sites of type X that interact with a given particle on a site of type Y ($X, Y \in \{A, B, O\}$). Simple counting yields

$$\begin{aligned} N_{O \rightarrow A} &= 1, \text{ by definition} \\ N_{A \rightarrow A} &= N + 4, \text{ interaction with } N - 2 \text{ on the line interacting with } O \\ &\quad \text{and intersection with } 2 \text{ } A \text{ s on the } 3 \text{ other lines} \\ N_{B \rightarrow A} &= 3N - 9, \text{ using } N_{O \rightarrow A} + N_{A \rightarrow A} + N_{B \rightarrow A} = 4N - 4 \\ N_{O \rightarrow B} &= 0, \text{ by definition} \\ N_{A \rightarrow B} &= 12, 4 \text{ lines with } 3 \text{ intersections each} \\ N_{B \rightarrow B} &= 4N - 16, \text{ using } N_{O \rightarrow A} + N_{A \rightarrow A} + N_{B \rightarrow A} = 4N - 4. \end{aligned} \quad (6)$$

The Boltzmann equations for the average number of particles in sites of types A and B are

$$\langle A \rangle = \lambda \exp(-(N + 4)\beta \langle A \rangle - (3N - 9)\beta \langle B \rangle - \beta) \quad (7)$$

and

$$\langle B \rangle = \lambda \exp(-12\beta \langle A \rangle - (4N - 16)\beta \langle B \rangle). \quad (8)$$

Here λ is a Lagrange multiplier factor enforcing the overall particle number to be N , i.e. so that

$$1 + 4(N - 1)\langle A \rangle + (N^2 - 4N + 3)\langle B \rangle = N \quad (9)$$

which simplifies to

$$4\langle A \rangle + (N - 3)\langle B \rangle = 1. \quad (10)$$

In the limit $N \rightarrow \infty$ one finds

$$\langle B \rangle = 1/N \quad \text{and} \quad \langle A \rangle = a/N \quad (11)$$

where a is finite. Consequently

$$\begin{aligned} \langle B \rangle &= \lambda \left(1 - \frac{a}{N}(1 - e^{-\beta})\right)^{12} \times \left(1 - \frac{1}{N}(1 - e^{-\beta})\right)^{4N-16} \\ &\rightarrow \lambda \exp(-4(1 - e^{-\beta})) \\ &= \frac{1}{N}. \end{aligned} \quad (12)$$

Hence

$$\lambda = \frac{1}{N} \exp(-4(1 - e^{-\beta})). \quad (13)$$

Taking similarly the large N limit for the equation for $\langle A \rangle$ yields

$$a = \exp((1 - e^{-\beta})(1 - a) - \beta) \quad (14)$$

and the energy E per particle is given by

$$E(\beta) = 2a(\beta). \quad (15)$$

For infinite temperature one finds that $E(0) = 2$ and for low temperatures $E(\beta) \sim 2e^{1-\beta}$. Hence, the mean-field calculation does not contradict the fact that there are zero-energy ground states for N prime.

3. The hypernetted chain approximation

Perhaps one of the most successful approximations in gas and liquid theory is the hypernetted chain (HNC) approximation [2], which is an integral equation which resums a certain class of diagrams in the virial expansion. Normally this integral equation must be resolved numerically and its resolution is rather difficult. However, we shall see here that for our model the resulting equation is drastically simplified in the large N limit.

The matrix form of the HNC equation is

$$\log(1 + h_{ij}) = -\beta V_{ij} + \rho \sum_k h_{ik}(h_{kj} - \log(1 + h_{kj}) - \beta V_{kj}) \quad (16)$$

where

$$h_{ij} = \frac{1}{\rho^2} (\langle \rho_i \rho_j \rangle - \rho \delta_{ij} - \rho^2). \quad (17)$$

Here ρ_i is the density at the site i and $\rho = \langle \rho \rangle$ in homogeneous systems. In this model $\rho = 1/N$. One may write the interaction matrix as

$$V_{ij} = 3\delta_{ij} + W_{ij}. \quad (18)$$

The important simplification comes from noting that (using the counting from the previous section)

$$W^2 = (3N - 9)I + (N - 6)W + 12U \quad (19)$$

where I is the identity matrix and U is the matrix with each element equal to 1. Also

$$U^2 = N^2U \quad \text{and} \quad UW = WU = (4N - 3)U. \quad (20)$$

Hence the elements W, I, U , form a closed algebra. In general we may therefore represent an element in this algebra by a triple

$$A \equiv (a_1, a_2, a_3) = a_3U + (a_2 - a_3)W + (a_1 - a_2)I \quad (21)$$

where

$$\begin{aligned} A_{ij} &= a_1 && \text{when } i = j \\ A_{ij} &= a_2 && \text{when } i \neq j \text{ and } V_{ij} = 1 \\ A_{ij} &= a_3 && \text{when } V_{ij} = 0. \end{aligned} \quad (22)$$

In this notation the product of two elements $A = (a_1, a_2, a_3)$ and $B = (b_1, b_2, b_3)$ is given by $C = AB = (c_1, c_2, c_3)$ where

$$\begin{aligned} c_1 &= a_3b_3N^2 + (a_1 - a_2)(b_1 - b_2) + (a_2 - a_3)(b_2 - b_3)(4N - 3) + (a_3(b_2 - b_3) \\ &\quad + b_3(a_2 - a_3))(4N - 3) + (a_3(b_1 - b_2) + b_3(a_1 - a_2)) \\ &\quad + ((a_1 - a_2)(b_2 - b_3) + (b_1 - b_2)(a_2 - a_3)) \end{aligned} \quad (23)$$

$$\begin{aligned} c_2 &= a_3b_3N^2 + (a_2 - a_3)(b_2 - b_3)(N + 6) + (a_3(b_2 - b_3) + b_3(a_2 - a_3))(4N - 3) \\ &\quad + (a_3(b_1 - b_2) + b_3(a_1 - a_2)) + ((a_1 - a_2)(b_2 - b_3) \\ &\quad + (b_1 - b_2)(a_2 - a_3)) \end{aligned} \quad (24)$$

and

$$c_3 = a_3 b_3 N^2 + 12(a_2 - a_3)(b_2 - b_3) + (a_3(b_2 - b_3) + b_3(a_2 - a_3))(4N - 3) + (a_3(b_1 - b_2) + b_3(a_1 - a_2)). \quad (25)$$

Using this algebra and taking the limit $N \rightarrow \infty$ at the end of the calculation one finds that, in this representation, the HNC reduces to

$$\log(1 + h_1) = -4\beta + \frac{4h_2^2 + h_3 - 7h_2h_3 + 3h_3^2}{1 + h_2 - h_3} \quad (26)$$

$$\log(1 + h_2) = -\beta + \frac{h_2^2 - h_2h_3 + h_3}{1 + h_2 - h_3} \quad (27)$$

and

$$\log(1 + h_3) = h_3. \quad (28)$$

The final equation is trivial giving $h_3 = 0$ and hence

$$h_1 = \exp\left(-4\beta + \frac{4h_2^2}{1 + h_2}\right) - 1 \quad (29)$$

with

$$\log(1 + h_2) = -\beta + \frac{h_2^2}{1 + h_2}. \quad (30)$$

For β small one finds $h_2 \sim -\beta$ and for β large $h_2 \sim -1 + 1/(\beta + 2 - \log(\beta) + O(\log(\beta)/\beta))$. The energy per particle is then given by

$$E = \frac{N}{2} \sum_{i=1}^{N^2} \langle \rho_0 \rho_i \rangle V_{0i} = 2(h_2 + 1). \quad (31)$$

Hence, at high temperatures, $E \sim 2(1 - \beta)$ as in the mean-field calculation, but $E \sim 2/(\beta + 2 - \log(\beta) + O(\log(\beta)/\beta))$ at low temperatures.

4. Monte Carlo simulation

The dynamics for the Hamiltonian (1) were simulated using a Monte Carlo method using the Metropolis algorithm with sequential update on the particles. Two variants of the dynamics have been analysed, first a non-local dynamics where a particle may move to any site on the board and secondly a local random walk dynamics where a particle may move to any of its eight nearest neighbours on the lattice. One of the advantages of the current model is that the energy may be expressed as a function of the occupation numbers of each row ($N_r(k)$), column ($N_c(k)$), left-to-right diagonal ($N_{d-}(k)$) and right-to-left diagonal ($N_{d+}(k)$). This greatly speeds up the calculation of the energy change at each move. In this notation it is easy to see that

$$E = \frac{1}{2N} \sum_{k=1}^N (N_r(k)^2 + N_c(k)^2 + N_{d-}(k)^2 + N_{d+}(k)^2) - 2. \quad (32)$$

This leads to a reduction by a factor of N of the time needed to compute the energy change with respect to a calculation using the particle positions. The form of the energy given by equation (32) demonstrates that if one was to neglect the diagonal interactions one would arrive at a model similar to two independent Backgammon models [4], but at negative temperature. The Hamiltonian is not strictly the same but the tendency is to put all the

particles in different boxes rather than to put them into a single box which is the ground state of the Backgammon model. Here the free-energy barriers clearly have an energetic component as opposed to the Backgammon model where their origin is entropic. We shall also see later that, similarly to the Backgammon model, the dynamical transition temperature appears to be at $T = 0$.

The system was started from a random initial configuration, thus simulating a rapid quench from high temperature to the simulation temperature. In both cases of non-local and local dynamics the energy as a function of time was measured.

In the case of non-local dynamics the particle–particle correlation function treating the particles as distinguishable is measured; it is defined by

$$C(t, t') = \frac{1}{N} \sum_i \delta_{x_i(t), x_i(t')} \delta_{y_i(t), y_i(t')} \quad (33)$$

note that C is normalized to be one when $t = t'$ (note that in keeping with convention, t' will always denote the earlier time). In the case of local dynamics it is interesting to measure the correlation function which gives us information about the effective particle diffusivities, this correlation function is normally denoted by $B(t, t')$ in the literature and is given by

$$B(t, t') = \frac{1}{N} \sum_i (x_i(t) - x_i(t'))^2. \quad (34)$$

We shall discuss the results of the two dynamic types separately.

4.1. Non local dynamics

With non-local dynamics one expects, at an intuitive level, that the dynamics should be faster and less prone to be glassy compared with local dynamics. If one imagines a self-consistent picture of a non-ordered phase, then a single particle moves in a potential generated by the other particles. When using non-local moves, trapping mechanisms at the spatial level are less important.

The simulations we carried out were for systems of 50 000 particles and times of up to 60 000 Monte Carlo sweeps through the entire system. In addition we verified that for systems of size 48 611 (which is prime) the results were not significantly altered.

Figure 1 shows the results of the energy per particle measured by the simulation for $t = 30\,000$. Up to values of $\beta = 5$ we found that by $t = 30\,000$ the energy density had reached a well-defined asymptotic value. We found for values of $\beta \geq 6$ that at $t = 30\,000$ the system had not reached an asymptotic value of the energy density and that the value of the energy density continued to decay very slowly. The values of E , shown on figure 1 for $\beta \geq 6$, are the values measured at $t = 30\,000$ and are not equilibrium values. One sees from figure 1 that between $\beta = 5$ and $\beta = 6$, the measured energy flattens off rather suddenly in a fashion reminiscent of glassy systems. For values of $\beta < 5$ and a minimum waiting time of 10 000 we found equilibrium behaviour for the correlation function. In this region

$$C(t, t') = C(t - t') \approx A \exp\left(-\frac{t - t'}{\tau_0}\right). \quad (35)$$

One may regard τ_0 as a characteristic timescale, if this timescale is greater than the observation time then one should expect out of equilibrium behaviour. Figure 2 shows a plot of $\log(\tau_0(\beta))$ as measured by fitting the simulation data with formula (35). As one can see, the plot is linear and the best fit is $\tau_0(\beta) = 0.317 \cdot \exp(1.796\beta)$; when β is such

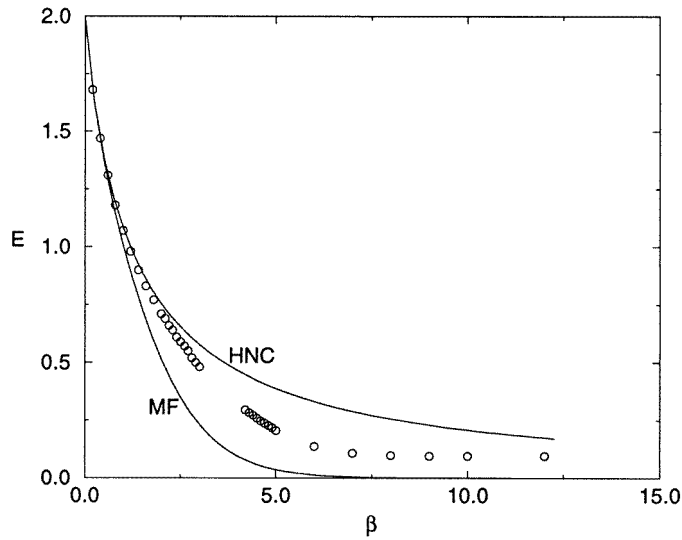


Figure 1. Non-local dynamics: dynamic energies for $L = 50\,000$ at $t = 30\,000$. Calculated static energies using the HNC and the mean-field approximation are also shown.

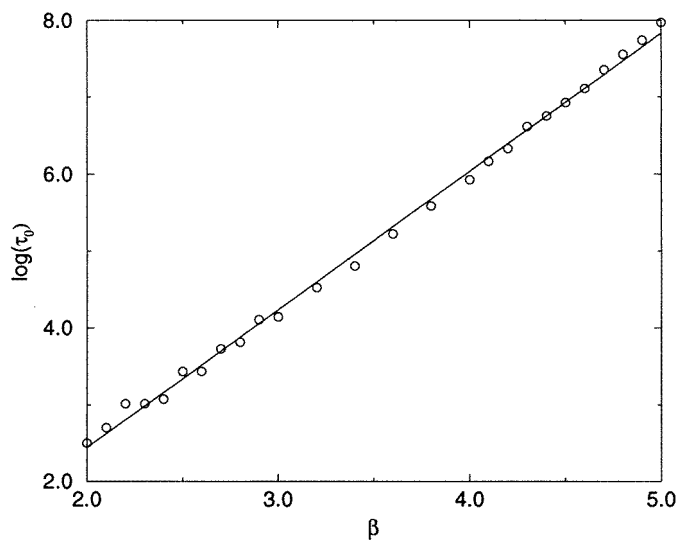


Figure 2. Non-local dynamics: $\log \tau_0(\beta)$ $L = 50\,000$ (with linear fit shown).

that $\tau_0(\beta)$ is much less than the age of the system one expects that equilibrium should be achieved. For an age of the system of order 10 000 one finds that the value of the temperature where the age and $\tau_0(\beta)$ have the same age is $\beta \approx 5.7$ which is entirely consistent with the plateau observed in the energy and with the breakdown of time translational invariance in the correlation function.

For values of $\beta \geq 6$ we found that the function $C(t, t')$ was no longer time translational invariant, neither did it have an exponential form. For values of $\beta \geq 7$ we found that to a reasonable degree of accuracy the system exhibits perfect ageing, i.e. $C(t, t') = f(t/t')$,

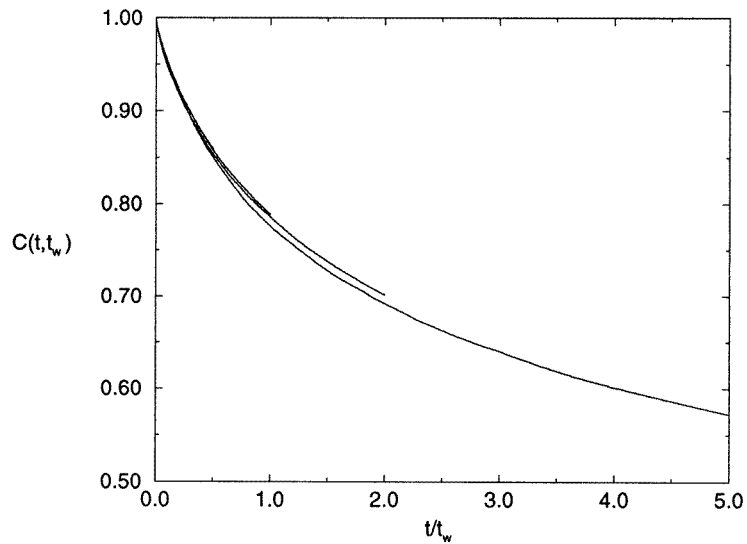


Figure 3. Non-local dynamics: $C(t, t_w)$ plotted against t/t_w at $\beta = 10$ for $t_w = 5000, 10000, 15000, 20000, 25000$ ($L = 50000$).

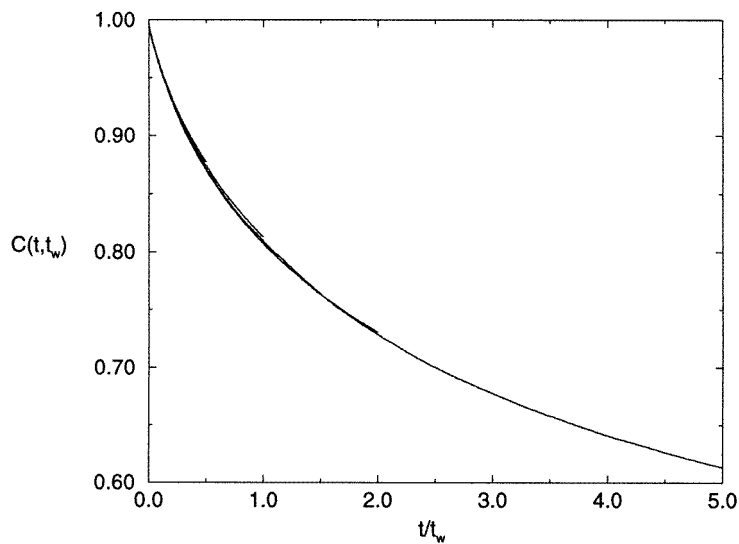


Figure 4. Non-local dynamics: $C(t, t_w)$ plotted against t/t_w at $T = 0$ for $t_w = 20000, 40000, 60000, 80000, 100000$ ($L = 50000$).

see for example the curves in figure 3 for $\beta = 10$. At $T = 0$ one sees that the system also ages and the five curves shown collapse onto the same master curve when plotted against t/t_w , this is shown in figure 4. Presumably this is because at $T = 0$ the characteristic time τ_0 becomes infinite and there is no interrupted ageing [6]. The scaling t/t' is observed in a variety of mean-field models [7] and also in the phenomenological trap model [8]. The improvement of the perfect ageing scaling as one approaches zero temperature was also observed by Ritort [4] in Monte Carlo simulations of the Backgammon model.

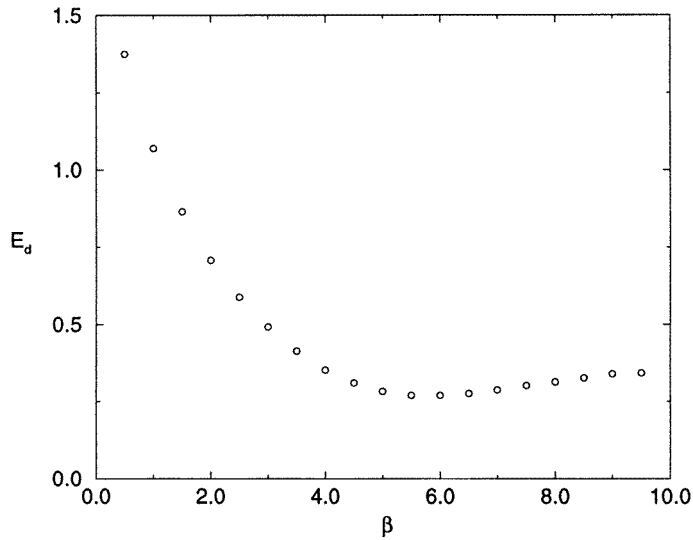


Figure 5. Local dynamics: dynamic energies for $L = 50\,000$ at $t = 2000$.

Finally, we mention here that in addition to simulations with $N = 48\,611$ particles we also carried out simulation with $N = 5000$ and $N = 4999$ particles to ensure that the energy density approaches a well-defined large N limit, thus justifying the restriction of our analysis of sections 2 and 3 to the case N odd.

4.2. Local dynamics

Here we consider the more physical situation of local random walk dynamics.

Figure 5 shows the energy measured for the local dynamics for a system of size 50 000 particles up to a time of 2000 Monte Carlo sweeps. Up to $\beta = 4$ the energy reaches an asymptotic value, where as for $\beta > 4$ the energy continues to decrease. The values shown in these cases are the minimum value of the energy attained. As one can clearly see from the figure, this measured value is not monotonic and actually increases after $\beta = 6.5$. For longer simulation times this minimum in the measured dynamic energy shifts towards larger values of β .

For values of the waiting time $t' = 10\,000, 20\,000, 30\,000, 40\,000$ up to $\beta = 4$ one sees that

$$B(t, t') = \kappa(\beta)(t - t') \quad (36)$$

and hence we are in an equilibrium phase for these temperatures and at this scale of age. The values of $\log(\kappa(\beta))$ are shown in figure 6; one sees that the curve is linear and one finds that $\kappa(\beta) = 0.34 \times \exp(-1.08\beta)$.

In the non-equilibrium regime we find that one may fit the curves as an anomalous diffusion but with a prefactor that depends on the waiting time. The behaviour of the particles is subdiffusive and we have fitted it with the form

$$B(t, t') = c(\beta) \frac{(t - t')^\alpha}{t'^\gamma} \quad (37)$$

where $\gamma = 2(1 - \alpha)$. This simple linear relation between the exponents for $(t - t')$ and t' works rather well but we have no theoretical reason to expect this result. An example of

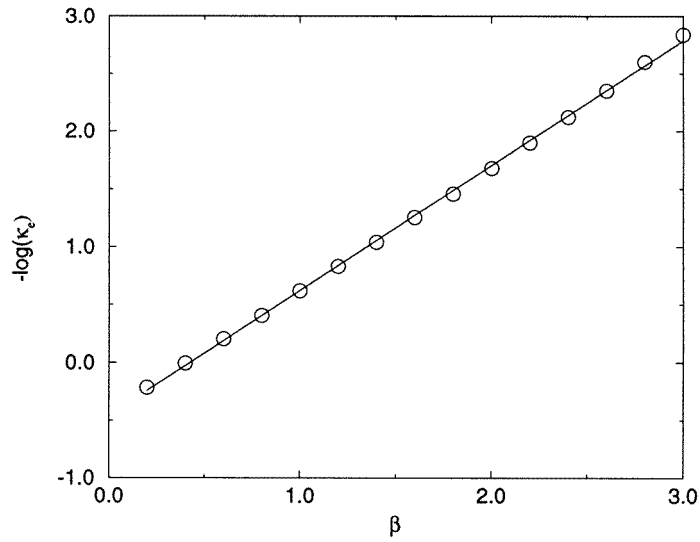


Figure 6. Local dynamics: $-\log(\kappa(\beta))$ in the equilibrium regime (with linear fit shown).

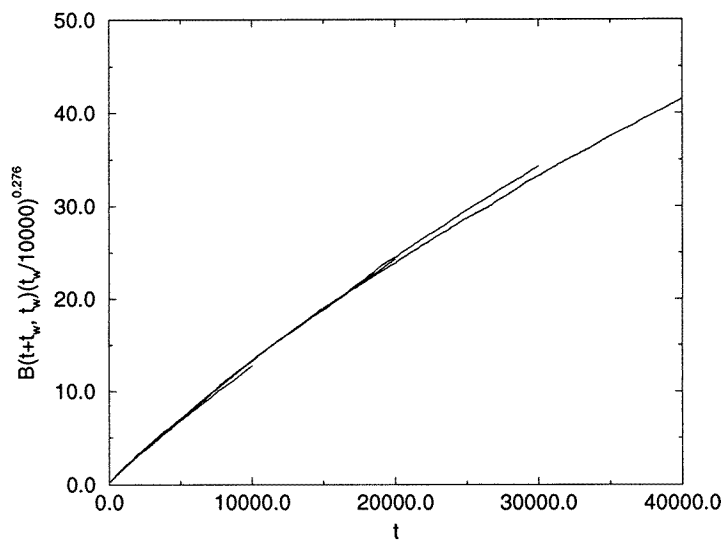


Figure 7. Local dynamics: rescaled $B(t + t_w, t_w)$ for $t_w = 10000, 20000, 30000, 40000$ at $\beta = 6$ with α taken to be 0.862.

the rescaled curves for $\beta = 6$ is shown in figure 6. The values of α as a function of β are shown in figure 7. To reach lower values of the temperature than those shown is rather difficult as the noise in the measured values of $B(t, t')$ becomes rather large, presumably because one is approaching the zero-temperature transition.

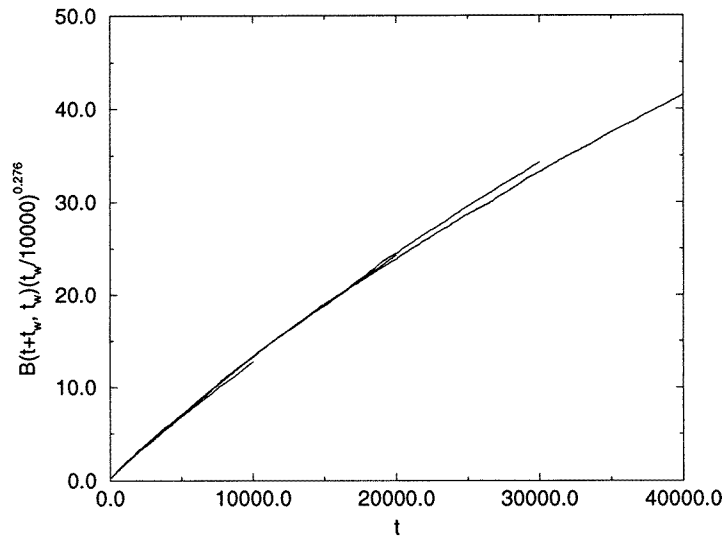


Figure 8. Local dynamics: $\alpha(\beta)$ in the non-equilibrium regime.

5. Conclusions

We have presented a preliminary study of a two-dimensional particle system which exhibits a dynamical transition between a gas/liquid and a glassy phase. As expected from the dynamical nature of the transition, the temperature at which one sees this transition is dependent on both the timescale of the observations and on the nature of the dynamics. The long-range nature of the interactions leads to a compact application of various standard approximation schemes for the statics—particularly the HCA which works reasonably well in the high-temperature phase. The model is also attractive from the simulation point of view, as the form of the interactions leads to an efficient implementation of the Monte Carlo updating procedure.

Acknowledgments

We would like to thank Lorenza and Leonardo Parisi for drawing our attention to the eight queens problem. We also thank Jérôme Houdayer and Olivier Martin for useful comments and their critical reading of the manuscript.

References

- [1] Götze W 1989 *Liquid, Freezing and Glass Transition (Les Houches Summer School)* ed J P Hansen, D Levesque and J Zinn-Justin (Amsterdam: North Holland)
- [2] Hansen J P and McDonald I R 1990 *Theory of Simple Liquids* (New York: Academic)
- [3] Mézard M and Parisi G 1996 *J. Phys. A: Math. Gen.* **29** 6515
- [4] Ritort F 1995 *Phys. Rev. Lett.* **75** 1190
- [5] Bouchaud J P, Cugliandolo L F, Kurchan J and Mézard M 1997 Out of equilibrium dynamics in spin-glasses and other glassy systems *Preprint cond-mat 9702070*; also in 1997 *Spin-glasses and Random Fields* ed A P Young (Singapore: World Scientific)
- [6] Bouchaud J P, Vincent E and Hammann J 1994 *J. Physique I* **4** 139
Cugliandolo L F and Dean D S 1995 *J. Phys. A: Math. Gen.* **28** 17

- [7] Cugliandolo L F and Kurchan J 1993 *Phys. Rev. Lett.* **71** 173
Franz S and Mézard M 1994 *Europhys. Lett.* **26** 209
Marinari E and Parisi G 1993 *J. Phys. A: Math. Gen.* **26** L1149
Cugliandolo L F and Dean D S 1995 *J. Phys. A: Math. Gen.* **28** 15
- [8] Bouchaud J P 1992 *J. Physique I* **2** 1705
Bouchaud J P and Dean D S 1995 *J. Physique I* **5** 265